Direction-Selective Resistance to Cerebrospinal-Fluid Flow As the Mechanism of Syrinx Generation in Syringomyelia

Han Soo Chang, M.D.

Department of Neurosurgery, Tokai University
Isehara, Japan

ABSTRACT

Example Abstract. Abstract must not include subheadings or citations. Example Abstract. Abstract must not include subheadings or citations. Example Abstract. Abstract must not include subheadings or citations. Example Abstract. Abstract must not include subheadings or citations. Example Abstract. Abstract must not include subheadings or citations. Example Abstract. Abstract must not include subheadings or citations. Example Abstract. Abstract must not include subheadings or citations.

Please note: Abbreviations should be introduced at the first mention in the main text no abbreviations lists. Suggested structure of main text (not enforced) is provided below.

Introduction

The pathophysiology of syringomyelia is still poorly understood. A number of hypotheses exist in the literature[1–13], but they provide widely different explanations on the mechanisms of syrinx generation. Most researchers, nevertheless, seem to agree on the following points. First, the syrinx fluid is identical to the CSF, and there should be some communication between the syrinx and the subarachnoid space. This point is supported by many studies[14–17], although a few different opinions exist[13,18]. Second, some derangement of CSF flow in the spinal subarachnoid space causes syrinx both in Chiari-I malformation[7,19–22] and subarachnoid arachnopathy[23–26]. The cerebellar tonsils hamper the CSF flow in the former and adhesive arachnoiditis in the latter.

The problem, however, is where this communicating channel resides and what mechanism generates the syrinx. On these points, there is no solid experimental or clinical evidence, and the opinions of researchers deviate widely. Gardner et al.[1] thought that the central canal intercommunicates the syrinx and the fourth ventricle, and arterial pressure waves exerted on the central canal generate the syrinx. Williams et al. also postulated the communication through the central canal, but for the syrinx generation mechanism, he emphasized the craniospinal pressure gradient produced by Valsalva maneuver et al[2].

On the other hand, Ball and Dayan[4] assumed that CSF enters the syrinx through the perivascular space of arteries penetrating the spinal cord. This idea has the following variations. Heiss et al.[7] proposed that the piston-like movement of the cerebellar tonsils in Chiari-I patients generates pressure waves in the spinal subarachnoid space, which subsequently drive CSF into the syrinx through the perivascular space. Stoodley et al. also considered the perivascular space as the communicating channel, but he assumed the arterial pulse pressure as the driving force of CSF[27] All these assumptions are not proven and remain hypothetical. Although the perivascular-space theory seems to be favored by recent researchers, there remains the possibility that a thin communicating channel exists between the syrinx and the fourth ventricle[28].

In our opinion, the main theoretical problems reside in the following points.

1. No theory can explain the pathophysiological mechanism of syringomyelia in a unified fashion.

2. No theory can explain how CSF enters from the low-pressure subarachnoid space to the high-pressure syrinx cavity and remains inside.

As to the first point, there are different syringomyelia types, such as Chiari-I-malformation and spinal-arachnopathy-related[23]. The Chiari-I-malformation-related syringomyelia is further divided into communicating and non-communicating[29]. For each of them, current theories assume a distinct mechanism of syrinx generation. However, it may be more natural to conjecture some common mechanism underlying these different types of syringomyelia[27]. The second point is theoretically

essential but challenging to solve. Physical theories dictate that the expanded syrinx cavity has higher pressure than the subarachnoid space[7,30–32]. Therefore, merely assuming a communicating channel does not explain how CSF enters the syrinx and remains inside against this pressure gradient. Even if we take a specific time window where the subarachnoid pressure exceeds the syrinx pressure, it does not explain how the CSF remains inside the syrinx after it.

The current article is part of our effort to solve the above theoretical problems. In our previous paper[28], we hypothesized that if there is a resistance to CSF flow in a particular direction (rostral or caudal), it causes a one-way valve-like effect on a CSF channel inside the spinal cord, leading to the accumulation of CSF and generation of a syrinx. This hypothesis was attractive to us because it could explain the pathophysiology of both Chiari-I-malformation-related syringomyelia and arachnopathy-related syringomyelia. Namely, in Chiari-I-malformation-related syringomyelia, the herniated cerebellar tonsils may function as a direction-selective resistance. In arachnopathy-related syringomyelia, some arachnoid adhesion may play the same function[26]. However, in that article, we just drew a rough sketch of this process and left out a detailed explanation. The current article will describe in detail how direction-selective resistance in the subarachnoid space generates a one-way valve mechanism in the CSF channel inside the spinal cord.

For this purpose, we used a mathematical model simulating the CSF movement of the spine—a revised version of our previous model[11,12]. This model describes the spinal CSF movement as an electric current in a modeled circuit (a lumped parameter model with multiple compartments[33]), and it assumes the existence of a patent central canal. We placed a direction-selective resistance in this model at a certain point in the spinal subarachnoid space and observed how it affects the CSF flow in the central canal.

Material and Method

Some problem exists in the computer simulation of the motion of biological fluids such as blood and CSF. Such bodily fluids move inside flexible tubes. It, therefore, requires different analysis techniques from those used in the engineering field, where the boundary of the conduit is supposed to be solid. For this purpose, researchers widely used lumped parameter models[?,33]. This model considers the fluid flow inside a flexible tube in analogy to the flow of electricity in an electric circuit. The accumulation of electricity in a capacitor represents the expansion of a flexible tube and the accompanying pressure elevation. An electrical resistor represents the frictional resistance to flow. This model has a wide variety. For example, it may model the whole cardiovascular system as one electric circuit, or it may model it as a synthesis of multiple compartments of electric circuits [@shi2011review; @kokalari2013review]. Our current model is the type of a lumped parameter model with multiple compartments. In this study, we did not intend to make a quantitatively precise model of the spinal CSF flow but to make a basic model that reveals the phenomenon underlying the generation of syringomyelia. For this purpose, we adopted a revised version of our previous lumped parameter model with multiple compartments.

Previously, we developed a mathematical model that simulated the CSF flow in the spine[11,12]. This model (a multiple-compartment version of a 1-dimensional lumped parameter model) could describe the CSF movement in the whole spine (Figure 1).

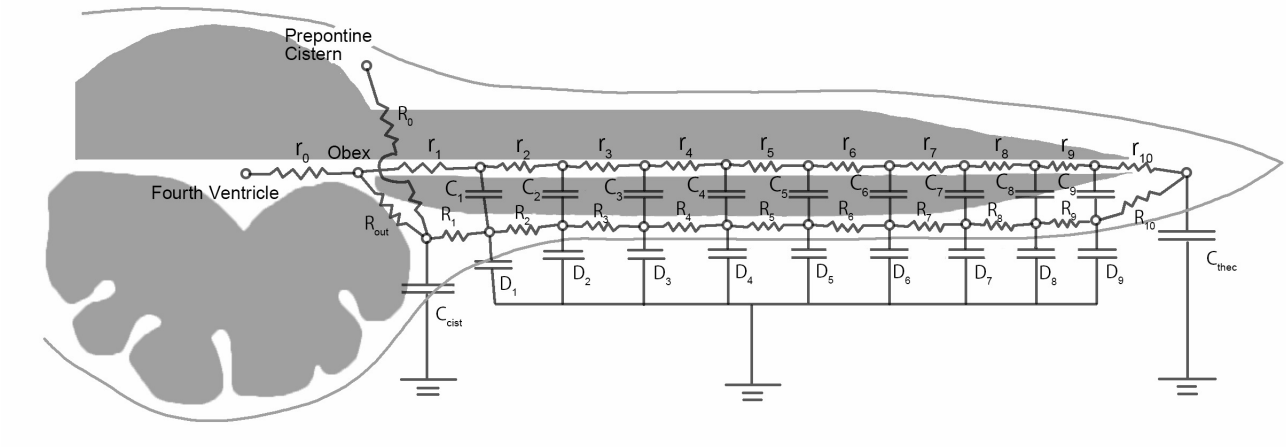

Figure 1. Schema of the electric circuit model of the CSF dynamics in the spine.

A set of differential equations can describe the behavior of this model. Using computer software, we can numerically calculate its behavior to a cranial pressure wave (defined as a boundary condition on the cranial points). This time, we

improved the previous model as follows.

- We increased the number of compartments from 10 to 100, thereby making the model more precise.
- We estimated the values of the parameters (the capacitance and resistance of each component) of the model as follows so that the model will become more realistic.
  - First, we set the length of the modeled spinal cord to be 1 meter.
  - The resistance of the subarachnoid space (R) was estimated using the following equations of Poisseuille[34–36].

$$\Delta P = \frac{8\pi\mu LQ}{A^2} = RQ$$

    * ΔP: Pressure difference between the adjacent compartments
    * Q: flow speed per unit surface
    * μ: viscosity coefficient. In this case, it was set to the value of water (0.0007).
    * L: distance between the adjacent compartments. It was set to 1 cm.
    * A: cross sectional area of the subarachnoid space. It was set to the value of a concentric annulus[36] with the outer diameter of 1cm and the inner diameter of 0.7 cm ($1.6 \times 10^{-4}(m^2)$)
  - Thus, R was calculated to be 6872 $(Pa \cdot sec/m^3)$
  - The resistance of the central canal (r) was estimated using the same equation with A set to $\pi(10^{-4})^2$ (m^2), i.e. the cross sectional area of a tube with a diameter of 100 μm. Thus, r was calculated to be 1.78×10^{11} $(Pa \cdot sec/m^3)$
- We determined the capacitance (C_{sub})corresponding to the dural elasticity so that the pressure-wave velocity determined by the time constant (RC) will roughly correspond to the pressure-wave velocity of the downward CSF wave observed in phase-contrast MRI of normal individuals. Thus, we set $C_{sub} = 0.1$ $(m^3/Pa \cdot sec)$.

Figure 1 shows the scheme of the constructed electric circuit model. This model represents the CSF movement in the spine as electric flow through multiple compartments of capacitances connected with resistors. Table 1 shows the values of the resistors and capacitors of the system. A set of differential equations can describe the behavior of this electric circuit, and we can solve it numerically by setting the voltage at the cranial nodes as the boundary condition (Figure 2). In the previous articles[11,12], we only analyzed the transient behavior of the model to a sudden pressure increase on the cranial side of the subarachnoid space. This analysis helped simulate the situation of coughing or Valsalva maneuvers. In this article, however, we analyzed the steady-state response of the model to an oscillating cranial pressure wave simulating the normal cardiac pulsation of the CSF.

We numerically solved the differential equations using computer software (Mathematica version 12, Wolfram Research, Champaign, IL, U.S.A.). We set the boundary conditions as follows. (1) The voltage at the two cranial nodes was set to a sine wave oscillating around 100 mmHg with an amplitude of 20 mmHg at one cycle per second. (2) The initial dural pressure was set at 100 mmHg in all segments. We set the step of the numerical solution to 1/5000 second and calculated the solution from zero to 20 seconds. We displayed the obtained solution as a movie in mp4 format.

Results

We present the system's responses as videos. Each video displays either all or some of the following four values simultaneously: namely, the dural tension (voltage in D capacitors in Figure 2), the canal tension (voltages in C capacitors), the subarachnoid CSF flow (flows in R resistors), and the canal flow (flows in r resistors). We plotted the node position on the x-axis and the values at that node on the y-axis. The pressure values are shown in cmH_2O, the flows in ml/sec. To plot different ranges of values in a single plot, we multiplied the following values with certain coefficients: namely, the canal tension with 50, the subarachnoid flow with 0.005, and the canal flow with 1.5×10^5. We plotted the rightward flow in the positive and the leftward flow in the negative direction. Video 1 shows the original system's response to the sine wave input on the cranial side. In this condition, CSF makes a smooth to-and-fro movement in the subarachnoid space with the corresponding pressure wave along the dura and the central canal. This response corresponds to the CSF dynamics in a normal individual.

In Video 2, we increased the subarachnoid resistance R_{25} by 20 times, thereby simulating a simple block of the subarachnoid flow in both directions. In this condition, the dural tension showed a pressure drop at node 25, corresponding to the

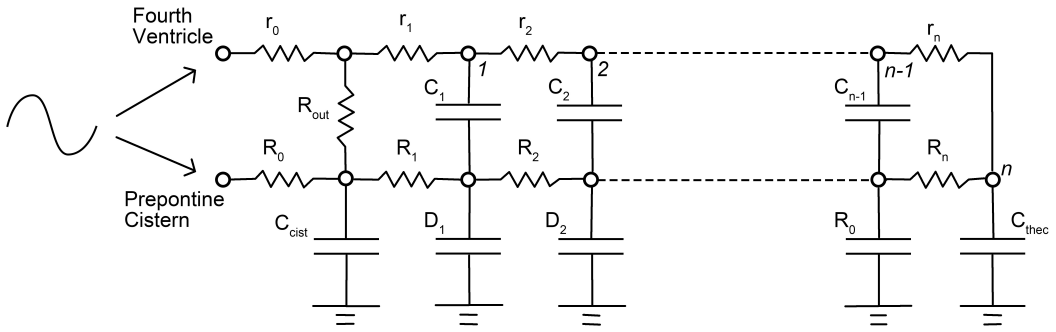

Figure 2. Electric circuit diagram representing the CSF dynamics of the spine

increased resistance both in caudal and rostral flow phases. This pressure drop caused an increase in canal flow in a direction identical to the subarachnoid CSF flow. This increased canal flow caused a transient increase in canal pressure distal to the block and a decrease proximal to the block. However, these pressure changes alternated according to the flow phase and did not produce a sustained condition. In Video 3, we replaced the subarachnoid resistor R_{25} with a one-way valve that selectively resisted flow in the caudal direction by 50 times. This time, the dural tension curve showed a pressure drop across node 25, appearing only during the caudal-flow phase. Canal flow showed alternating increase in caudal and rostral directions according to the flow phase, which was similar to that in the simple block above. However, there was a significant difference. Sustained high pressure appeared in the central canal distal to the valve, and some sustained low pressure in the segment proximal to the valve. The canal flow near node 25 markedly increased caudally in the caudal-flow phase and rostrally in the rostral-flow phase. We took out the canal flow and showed it in Video 4. Observing this video, we can see that the cumulative total of the caudal flow is larger than that of the rostral flow, and it means that the CSF is virtually pumped caudally at node 25.

Discussion

In this article, we theoretically analyzed the CSF movement in the spinal cord using a lumped parameter model with multiple components. It simulated a system with an elastic tube (dura) containing an elastic cylindrical material (spinal cord) that itself contained a fluid channel (the central canal). When we placed a direction-selective resistor in the subarachnoid channel and evoked a to-and-fro pressure wave on this system, it produced a sustained pressure elevation in the segment distal to the direction-selective resistor. This phenomenon may explain the pathogenesis of syringomyelia both in Chiari I malformation and syringomyelia associated with arachnopathy.

Subarachnoid pressure affects the pressure inside the central canal. As seen in Figure 2, the absolute pressure inside the central canal is the sum of the subarachnoid and canal pressure (voltages of C_k and D_k in electrical terms). Suppose a one-way valve selectively resists caudal flow in the subarachnoid space at point A, and CSF makes a to-and-fro movement across it. The caudal-flow phase creates a pressure drop across point A, making the subarachnoid pressure in the distal segment smaller, and it reduces the absolute canal pressure in the distal segment. Thus, the pressure gradient in the central canal across point A increases, which increases the distal CSF flow in the canal at that point.

On the contrary, the rostral flow does not create a pressure drop. Although some of the CSF pumped caudally will flow back rostrally, its amount will be smaller. The net result will be that some CSF is pumped caudally in one cycle of the to-and-fro movement. Thus, CSF gradually accumulates in the distal segment of the resistance. We hypothesize that this is the

mechanism underlying the syrinx generation.

This hypothesis solves the theoretical problems pointed out in the Introduction. A one-way valve in subarachnoid space creates an asymmetry of the pressure gradient between the caudal and rostral flow phases in the central canal. This asymmetric alternation of pressure gradient effectively pumps CSF caudally, creating sustained pressure elevation in the caudal segment. In other words, the energy of the to-and-fro CSF movement is translated via the one-way valve into the creation and sustenance of syringomyelia.

Direction-selective resistance to CSF flow is not an imaginative assumption but actually exists in patients. In Chiari-I malformation, the herniated tonsils move like a ball-valve, displaced caudally during the caudal flow and rostrally during the rostral flow. Higher velocity observed in the phase-contrast MRI studies suggests that it selectively impedes the caudal CSF flow more than the cranial flow. This direction-selective resistance was demonstrated by Williams in direct measurements in Chiari-I patients and became the basis of his theory[37].

Also, there is a possibility that some types of arachnoid pathology function as one-way valves. In 2014, we reported a case of thoracic arachnoid web associated with syringomyelia, in which phase-contrast MRI detected one-way-valve-like behavior of the arachnoid web[26]. We found an obliquely oriented arachnoid web that reminded us of a one-way valve in surgery. Thus, our hypothesis may also solve the second theoretical problem that we pointed out in the Introduction. Namely, we may consider the presence of a one-way valve in spinal subarachnoid space as a common mechanism underlying both Chiari-I-related and arachnopathy-related syringomyelia. Our theory assumes that the arterial-pulse generated to-and-fro CSF movement provides the energy for syrinx generation. It is compatible with Stoodley et al.'s experimental result that syrinx maintenance is dependent on arterial pulsation[27]. In this study, the authors showed that

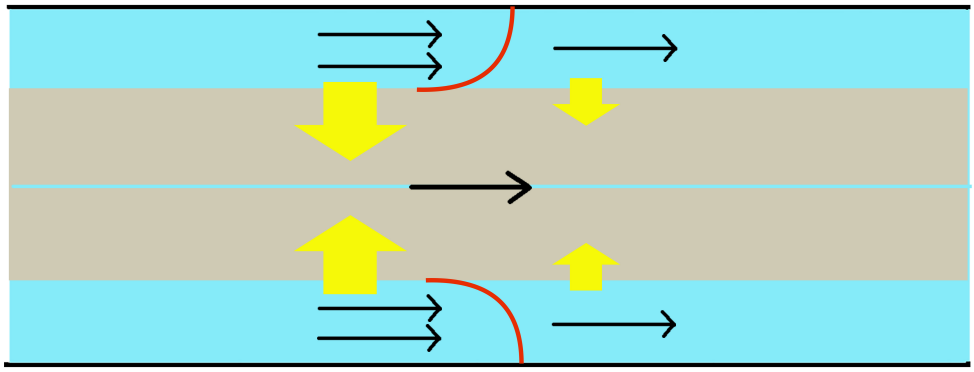

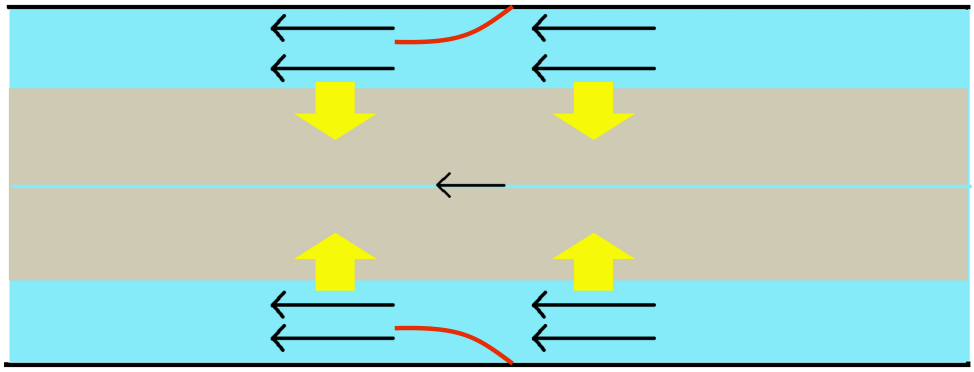

References

1. Gardner, W. J. & Angel, J. The mechanism of syringomyelia and its surgical correction. *Clin Neurosurg.* **6**, 131–40 (1958).
2. Williams, B. On the pathogenesis of syringomyelia: A review. *J. Royal Soc. Medicine* **73**, 798–806 (1980).
3. Milhorat, T. H. *et al.* Chiari I malformation redefined: Clinical and radiographic findings for 364 symptomatic patients. *Neurosurgery* **44**, 1005–1017, DOI: 10.1097/00006123-199905000-00042 (1999).
4. Ball, M. J. & Dayan, A. D. Pathogenesis of syringomyelia. *Lancet (London, England)* **2**, 799–801, DOI: 10.1016/s0140-6736(72)92152-6 (1972).
5. Klekamp, J. The pathophysiology of syringomyelia - historical overview and current concept. *Acta Neurochir.* **144**, 649–664, DOI: 10.1007/s00701-002-0944-3 (2002).
6. du Boulay, G., Shah, S. H., Currie, J. C. & Logue, V. The mechanism of hydromyelia in Chiari type 1 malformations. *The Br. J. Radiol.* **47**, 579–587, DOI: 10.1259/0007-1285-47-561-579 (1974).
7. Heiss, J. D. *et al.* Elucidating the pathophysiology of syringomyelia. *J. Neurosurg.* **91**, 553–562, DOI: 10.3171/jns.1999.91.4.0553 (1999).
8. Milhorat, T. H., Miller, J. I., Johnson, W. D., Adler, D. E. & Heger, I. M. Anatomical basis of syringomyelia occurring with hindbrain lesions. *Neurosurgery* **32**, 748–754; discussion 754, DOI: 10.1227/00006123-199305000-00008 (1993).
9. Stoodley, M. A. Pathophysiology of syringomyelia. *J. Neurosurg.* **92**, 1069–1070; author reply 1071–1073 (2000).
10. Terae, S., Miyasaka, K., Abe, S., Abe, H. & Tashiro, K. Increased pulsatile movement of the hindbrain in syringomyelia associated with the Chiari malformation: Cine-MRI with presaturation bolus tracking. *Neuroradiology* **36**, 125–129 (1994).
11. Chang, H. S. & Nakagawa, H. Hypothesis on the pathophysiology of syringomyelia based on simulation of cerebrospinal fluid dynamics. *J. Neurol. Neurosurgery, Psychiatry* **74**, 344–347 (2003).
12. Chang, H. S. & Nakagawa, H. Theoretical analysis of the pathophysiology of syringomyelia associated with adhesive arachnoiditis. *J. Neurol. Neurosurgery, Psychiatry* **75**, 754–757 (2004).
13. Greitz, D. Unraveling the riddle of syringomyelia. *Neurosurg. Rev.* **29**, 251–263; discussion 264, DOI: 10.1007/s10143-006-0029-5 (2006).

14. Ellertsson, A. B. Syringomyelia and other cystic spinal cord lesions. *Acta Neurol. Scand.* **45**, 403–417, DOI: 10.1111/j.1600-0404.1969.tb01254.x (1969).

15. Ellertsson, A. B. & Greitz, T. Myelocystographic and fluorescein studies to demonstrate communication between intramedullary cysts and the cerebrospinal fluid space. *Acta Neurol. Scand.* **45**, 418–430 (1969).

16. Li, K. C. & Chui, M. C. Conventional and CT metrizamide myelography in Arnold-Chiari I malformation and syringomyelia. *AJNR. Am. journal neuroradiology* **8**, 11–17 (1987 Jan-Feb).

17. Heiss, J. D. *et al.* Origin of Syrinx Fluid in Syringomyelia: A Physiological Study. *Neurosurgery* **84**, 457–468, DOI: 10.1093/neuros/nyy072 (2019).

18. Koyanagi, I. *et al.* Surgical treatment supposed natural history of the tethered cord with occult spinal dysraphism. *Child's Nerv. Syst. ChNS: Off. J. Int. Soc. for Pediatr. Neurosurg.* **13**, 268–274, DOI: 10.1007/s003810050081 (1997).

19. Wolpert, S. M., Bhadelia, R. A., Bogdan, A. R. & Cohen, A. R. Chiari I malformations: Assessment with phase-contrast velocity MR. *AJNR. Am. journal neuroradiology* **15**, 1299–1308 (1994).

20. Bhadelia, R. A. *et al.* Cerebrospinal fluid flow waveforms: Analysis in patients with Chiari I malformation by means of gated phase-contrast MR imaging velocity measurements. *Radiology* **196**, 195–202, DOI: 10.1148/radiology.196.1.7784567 (1995).

21. Hofmann, E., Warmuth-Metz, M., Bendszus, M. & Solymosi, L. Phase-contrast MR imaging of the cervical CSF and spinal cord: Volumetric motion analysis in patients with Chiari I malformation. *AJNR. Am. journal neuroradiology* **21**, 151–158 (2000).

22. Quigley, M. F., Iskandar, B., Quigley, M. E., Nicosia, M. & Haughton, V. Cerebrospinal fluid flow in foramen magnum: Temporal and spatial patterns at MR imaging in volunteers and in patients with Chiari I malformation. *Radiology* **232**, 229–236, DOI: 10.1148/radiol.2321030666 (2004).

23. Klekamp, J., Batzdorf, U., Samii, M. & Bothe, H. W. Treatment of syringomyelia associated with arachnoid scarring caused by arachnoiditis or trauma. *J. Neurosurg.* **86**, 233–240, DOI: 10.3171/jns.1997.86.2.0233 (1997).

24. Brodbelt, A. R. *et al.* Altered subarachnoid space compliance and fluid flow in an animal model of posttraumatic syringomyelia. *Spine* **28**, E413–419, DOI: 10.1097/01.BRS.0000092346.83686.B9 (2003).

25. Heiss, J. D. *et al.* Pathophysiology of primary spinal syringomyelia. *J. Neurosurgery. Spine* **17**, 367–380, DOI: 10.3171/2012.8.SPINE111059 (2012).

26. Chang, H. S., Nagai, A., Oya, S. & Matsui, T. Dorsal spinal arachnoid web diagnosed with the quantitative measurement of cerebrospinal fluid flow on magnetic resonance imaging. *J. Neurosurgery. Spine* **20**, 227–233, DOI: 10.3171/2013.10.SPINE13395 (2014).

27. Stoodley, M. A., Jones, N. R., Yang, L. & Brown, C. J. Mechanisms underlying the formation and enlargement of noncommunicating syringomyelia: Experimental studies. *Neurosurg. Focus.* **8**, 1–7, DOI: 10.3171/foc.2000.8.3.2 (2000).

28. Chang, H. S. Hypothesis on the pathophysiology of syringomyelia based on analysis of phase-contrast magnetic resonance imaging of Chiari-I malformation patients, DOI: 10.12688/f1000research.72823.1 (2021).

29. Elliott, N. S. J., Bertram, C. D., Martin, B. A. & Brodbelt, A. R. Syringomyelia: A review of the biomechanics. *J. Fluids Struct.* **40**, 1–24, DOI: 10.1016/j.jfluidstructs.2013.01.010 (2013).

30. Serway, R. A. Fluids and Solids. In *College Physics*, 267–319 (Cengage Learning, Boston, 2016), eleventh edn.

31. Davis, C. H. & Symon, L. Mechanisms and treatment in post-traumatic syringomyelia. *Br. J. Neurosurg.* **3**, 669–674, DOI: 10.3109/02688698908992690 (1989).

32. Ellertsson, A. B. & Greitz, T. The distending force in the production of communicating syringomyelia. *Lancet (London, England)* **1**, 1234, DOI: 10.1016/s0140-6736(70)91829-5 (1970).

33. Shi, Y., Lawford, P. & Hose, R. Review of Zero-D and 1-D Models of Blood Flow in the Cardiovascular System. *BioMedical Eng. OnLine* **10**, 33, DOI: 10.1186/1475-925X-10-33 (2011).

34. Brook, B. S., Falle, S. & Pedley, T. J. Numerical solutions for unsteady gravity-driven flows in collapsible tubes: Evolution and roll-wave instability of a steady state. *J. Fluid Mech.* **396**, 223–256 (1999).

35. Sherwin, S. J., Formaggia, L., Peiro, J. & Franke, V. Computational modelling of 1D blood flow with variable mechanical properties and its application to the simulation of wave propagation in the human arterial system. *Int. journal for numerical methods fluids* **43**, 673–700 (2003).

36. Huilgol, R. R. & Georgiou, G. C. A fast numerical scheme for the Poiseuille flow in a concentric annulus. *J. Non-Newtonian Fluid Mech.* **285**, 104401, DOI: 10.1016/j.jnnfm.2020.104401 (11 1, 2020).

37. Williams, B. Simultaneous cerebral and spinal fluid pressure recordings. 2. Cerebrospinal dissociation with lesions at the foramen magnum. *Acta Neurochir.* **59**, 123–142, DOI: 10.1007/BF01411198 (1981).